

The Use of Latex Rubber-Modified Polystyrene as a Model System for HIPS: Effect of Particle Size

D. G. COOK,¹ A. RUDIN,^{1,*} and A. PLUMTREE²

¹Department of Chemical Engineering, Institute for Polymer Research, University of Waterloo, Waterloo, Ontario, Canada N2L 3G1; ²Department of Mechanical Engineering, Institute for Polymer Research, University of Waterloo, Waterloo, Ontario, Canada N2L 3G1

SYNOPSIS

The effect of particle size in high-impact polystyrene (HIPS) is difficult to determine because of a size polydispersity and changes in particle morphology during the HIPS synthesis process. In this study, poly(*n*-butyl acrylate) rubber core/polystyrene shell particles were made by emulsion polymerization methods such that the only difference was in particle diameter, which ranged from 0.4 to 6.2 μm . The latexes were subsequently incorporated into a polystyrene matrix to form a toughened composite that acted as a simple model for HIPS. Charpy impact energies (notched and unnotched) of the composites showed that there was no toughening for particle sizes less than 2 μm in diameter. The optimal impact energy was obtained with particle diameters in the region of 2–3 μm at 8 wt % rubber loading. The results imply that craze stabilization is the most important aspect of the toughening process. A simple toughening model based on the crack opening displacement of craze breakdown between adjacent rubber particles is suggested, with interparticle distance as the most important variable. © 1993 John Wiley & Sons, Inc.

INTRODUCTION

In rubber-toughened polymers, there are many factors that determine the degree of toughening including rubber/matrix adhesion, rubber particle size and size distribution, rubber content and phase volume, relaxation behavior of rubber (modulus and T_g), and composition of matrix.¹ In solution-polymerized materials such as high-impact polystyrene (HIPS), it is difficult to separate these variables and thus determine the true effect of a given factor. Nevertheless, an understanding of the most general aspects of the toughening in HIPS has been established from the work of Bucknall and co-workers^{2,3} and others.⁴ The mechanism is a two-step process involving

1. Formation of massive crazing within the polystyrene matrix. The strain energy ab-

sorbed is directly proportional to the degree of crazing.

2. Control of craze breakdown to avoid premature failure. Crazes can degenerate into a running crack, resulting in matrix failure.

In HIPS, the formation of crazes is enhanced by rubber particles that increase the local stress at the equator of the particle to approximately twice the nominal stress.⁵ As a consequence, massive crazing throughout the matrix is initiated at these interfaces and the applied deformational energy is dissipated. However, glass particles embedded in polystyrene will initiate an equally high number of crazes and the fact that this type of material does not have any significant impact toughness⁶ demonstrates that the second step is an important consideration. Unfortunately, while much research has concentrated on the first step, relatively little is known about the latter.

With respect to particle size, previous work⁷ on HIPS has shown that there is an optimum size in

* To whom correspondence should be addressed.

the region of 1–4 μm for maximum toughness. Since HIPS has a broad distribution of particle sizes and the internal particle morphology often changes with size, the effect of particle size is difficult to isolate. In the work detailed here, rubber particles are made using emulsion polymerization techniques and compounded into polystyrene to form a toughened composite. The particle has a layered structure, with a poly(*n*-butyl acrylate) rubber core and polystyrene outer shell for compatibilization with the matrix.

The concept of using latex particles to toughen polymers is not new and is the basis of toughened poly(methyl methacrylate) and ABS. As noted, however, polystyrene requires rubber particles 1 μm or larger for effective toughening and this is not typically the range for emulsion polymerization. The specialized techniques employed here allow creation of monodisperse particles up to 7 μm .⁸ Certainly, core-shell materials are not optimal for toughening polystyrene⁹ since high-phase volume, grafting between the rubber and matrix, and complex rubber particles cannot be met with this method at present; these parameters are highly developed in commercial HIPS. However, the system presented here is very simple, and therein lies its attraction. As much as possible, all variables are kept constant except for particle size, and so the true effect of this variable can be determined.

EXPERIMENTAL

The preparation method of the poly(*n*-butyl acrylate) core/polystyrene shell latex particles is detailed elsewhere.⁸ Briefly, the rubber cores were prepared by layered buildup of poly(*n*-butyl acrylate) until the desired diameter was reached. This was followed by a final 0.1 μm thick shell of polystyrene. Both the rubber core and outer polystyrene shell were lightly cross-linked so that the particles could survive melt-blending operations. A typical scanning electron micrograph is shown in Figure 1 for 6 μm particles, displaying their uniform shape and size. A few secondary particles were also created during synthesis, but these were kept at a minimum by the proper choice of reaction conditions. The particle diameter and polydispersity of the core-shell latexes prepared are shown in Table I.

After preparation, the latex was coagulated. Gross amounts of water were drawn off and the separated latex dried in a vacuum oven at 70°C and –30 in. Hg for 24 h. The dried material was frozen in liquid nitrogen and then broken up in a shredding mill. The powdered latex was mixed with a crystal polystyrene ($M_n = 85,000$; $M_w = 242,000$; $M_z = 408,000$) and melt-blended on a Leistritz ZSK 34 corotating twin screw extruder with four kneading zones and vacuum extraction. The amount of latex was varied

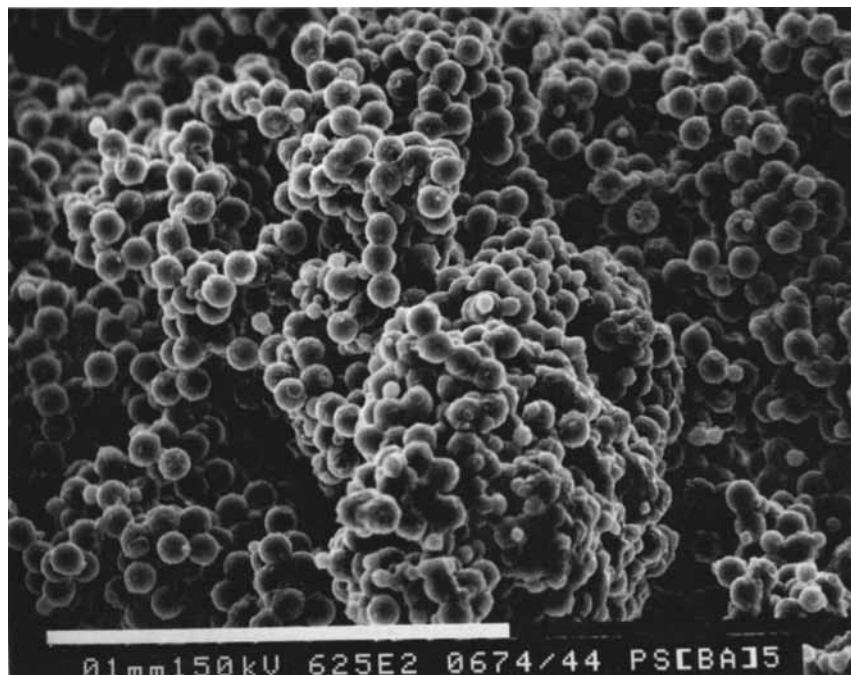


Figure 1 SEM photograph of 6 μm core-shell latex particles, showing regular morphology and some secondary particles. The scale (white bar) is 0.1 mm in length.

Table I Poly(*n*-Butyl Acrylate) Core-Polystyrene Shell Latexes

Material	Rubber Core Diameter (μm)	Polydispersity, (D_w/D_n)
PSBA-159	0.44	1.007
PSBA2-146	0.91	1.005
PSBA2-164	1.2	1.004
PSBA3-165	2.4	1.011
PSBA4-163	3.7	1.004
PSBA5-162	6.2	1.01

D_n = number-average particle diameter; D_w = weight-average particle diameter.

to obtain different volume fractions of rubber (2–8%) in the composite. Because the particles have a solid rubber core and both the rubber and polystyrene have the same density, the rubber phase volume is the same as the rubber weight percent in the composite.

The extruded composites were molded on a Battenfeld Unilog 1000 injection molder to form standard ASTM half-Charpy bars ($12.6 \times 6.6 \times 75$ mm). The bars were annealed at 95–98°C for 18–24 h and then left for 1 day at room temperature. Impact energy was determined on an instrumented Charpy

testing apparatus.¹⁰ An impact velocity of 1 m/s was used for 2.5 mm notched bars and a 2 m/s velocity for the unnotched specimens.

RESULTS

Observations and Discussion

The effect of particle size on notched and unnotched Charpy impact energy for an 8 wt % rubber blend is shown in Figure 2. The results for both tests showed the same trend. Figure 2 clearly shows that there is an optimal toughness in the 2–3 μm region. There is no significant toughness increase over that of the matrix for smaller particle diameters, whereas after the optimum, the impact energy decreases slowly with increasing particle size.

The results shown here are very similar to data obtained by Wrotecki et al.¹¹ for poly (methyl methacrylate) in which the optimal particle diameter was about 0.3 μm . There was little impact improvement at smaller particle diameters and the toughness decreased monotonically for larger particles. Generally, it has been noted that the minimum particle diameter for toughening of crazing polymers is one approximately equal to or larger than the craze

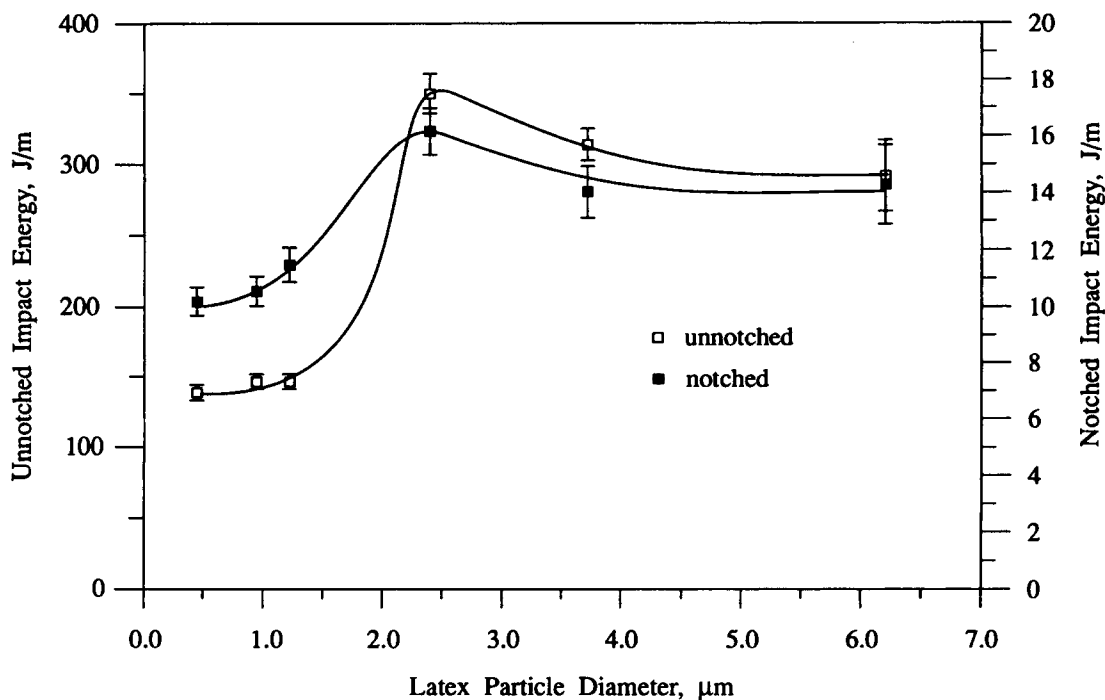


Figure 2 Impact energy (J/m) vs. latex particle diameter (μm) for notched and unnotched Charpy bars for 8 rubber wt % composites. Errors bars in data represent 95% confidence limit.

thickness in the matrix.⁴ For polystyrene, the maximum craze thickness is about 1–2 μm ,¹² whereas for poly(methyl methacrylate), the size is much less than 1 μm .

Recently, the work by Wu¹³ has been used as a rationale for particle-size effects in rubber-toughened materials. He investigated the effect of particle diameter in nylon–rubber blends and found that impact energy decreased markedly as particle size increased for a constant rubber volume. From this, Wu suggested that the particle spacing must not exceed a critical distance for optimal toughness. While some researchers^{14,15} have used this approach for HIPS, the Wu model was developed for shear yielding polymers, not crazing polymers. The present results confirm this difference in that very small rubber particles are ineffective in toughening the polystyrene matrix, whereas Wu's work demonstrates that the smallest diameter rubber particles appear to be the most effective in shear yielding polymers such as nylon.

Although the Goodier equations⁵ predict that particle size is not a factor in stress enhancement at the particle/matrix interface, Donald and Kramer¹⁶ showed that crazes rarely nucleated from particles of less than 1 μm in diameter in HIPS. This was explained by a drop in the stress enhancement by a factor of $(R/x)^5$, where x is the distance from the matrix–particle interface and R is the particle radius. Since the crazing region in polystyrene must be initiated approximately 3 fibril spacings or about 75 nm from the surface of the particle,¹⁷ it was argued that the particles must be larger than 1 μm in diameter for effective craze nucleation.

Whether or not small particles can nucleate crazes is controversial. Okamoto et al.¹⁸ showed evidence of craze initiation from submicron particles during the fracture process, and Grocela and Nauman¹⁴ found that submicron particles could toughen polystyrene. The most reasonable explanation is that as polystyrene approaches the nominal crazing stress during a fracture event craze initiation will occur from smaller particles. In a mixture of particle sizes, an extensive craze network would be established initially by the larger particles, but smaller particles would initiate crazes as the stress increased to the craze stress of the matrix.

Donald and Kramer¹⁹ also speculated that the toughening process might be dependent on internal particle morphology. Smaller particles are more likely to be solid rubber and thus easily debond or cavitate, creating voids in the matrix that would be ineffective in stabilizing the craze. However, the present results show that solid rubber particles larger

than 2 μm remain much more effective in toughening compared to smaller particles.

The breaking stress and strain for unnotched Charpy tests are shown in Table II for the various particle sizes and the polystyrene matrix. Also included are values for a typical HIPS material. The results indicate that besides a higher strain to fracture the tougher (i.e., $\geq 2 \mu\text{m}$ particle blends and HIPS) materials support a higher stress before breakage compared to the lower toughness materials ($< 2 \mu\text{m}$ particle blends and matrix polystyrene). This is at variance with the assumption²⁰ that the rubber particles in HIPS increase the crazing rate at a lower applied tensile stress, and as a result, the total stress field is kept below the critical level for crack formation by flaws such as dust particles within the matrix. Thus, effectively toughened blends should fail at a stress no higher than that of the matrix polystyrene. Since this is not the case, then it is implied that the crazes formed at the particle/matrix interface are prevented from prematurely breaking down into cracks, even at the higher tensile stress experienced.

The ability to support a higher stress at breakage is important. Creep experiments by Bucknall and Clayton²¹ showed that the crazing rate is a function of the stress in excess of the crazing initiation stress. Thus, under impact, the stress increases until the volume change rate due to crazing matches the deformation rate. If the material can stabilize the crazes formed, then the part will survive. If on the other hand there is no craze stability, then the crazes will quickly degenerate into cracks and the load is

Table II Stress and Strain at Fracture for Unnotched Charpy Bars with 8 Wt % Latex Rubber

Particle Diameter (μm)	Stress (Mn/m^2)	Strain (%)
None ^a	52.7	5.42
0.44	59.4	7.05
0.91	60.5	7.10
1.2	55.3	6.40
2.4	70.8	11.7
3.7	70.2	10.8
5.7	66.5	9.6
	67.9	10.5
HIPS ^b	68.1	18.36

^a Matrix polystyrene alone. The approximate crazing stress for the matrix polystyrene is 53 MN/m^2 at high strain rates (50 s^{-1}).¹⁰

^b 4% rubber content; 10–20% phase volume.

carried by the remainder of the section, resulting in matrix failure. Conversely, at low strain rates, the fracture stress for HIPS is significantly lower than that of polystyrene, as shown by tensile experiments.²² The deformation rate for these conditions is sufficiently slow so that only a low stress is needed to maintain the crazing rate necessary for deformation.

Thus, it would appear that the delay of fracture of the craze formed is the most important aspect of the toughening mechanism for these materials under high-speed impact. Argon²⁰ has used an analogous argument to produce toughened polystyrene by the addition of submicron-sized reservoirs of low molecular weight rubber to a polystyrene matrix. The reservoirs are broken by nearby crazes and the rubber plasticizes the craze fibrils, allowing them to draw out more fully and so match the applied deformation rate. Thus, the fibril stability is enhanced and fibril breakdown resulting in the ultimate breakdown of the matrix is delayed. The actual initiation of crazes is of secondary importance.

Proposed Craze Breakdown Model

It is assumed that breakdown of the craze occurs by the mechanisms proposed by Hull.²³ In this model, once the highly extended craze fibrils fracture, a void is formed, creating a stress concentration, and the ensuing crack proceeds down the center of the craze. Computer modeling by Hobbs²⁴ showed that the fracture of HIPS could be described if crazes exceeded a critical length and that the fracture could

be contained if the crazes were “pinned” between large particles, although no mechanism was offered for the actual process of controlling the crazes.

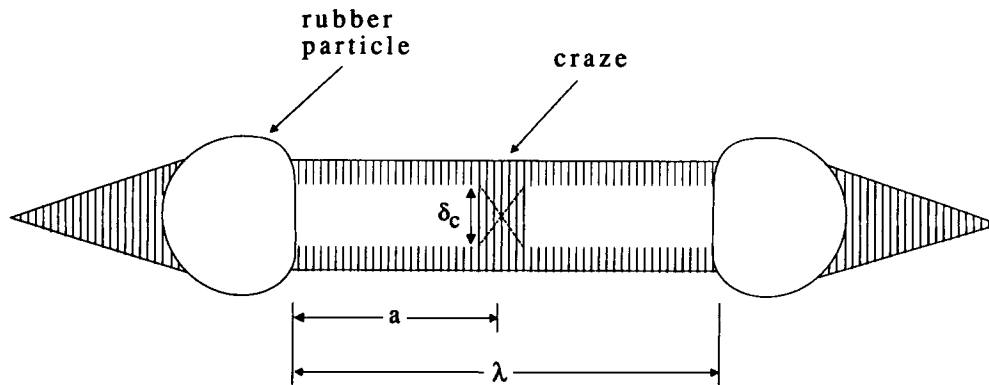
In effect, the rubber particles serve to act as barriers for crazes running between them. The ability to act as a barrier depends on particle size, rubber/matrix adhesion, particle morphology, and other factors. During craze breakdown, a crack occurs in a craze between adjacent particles. Since the particles continue to enhance the stress even after crazing has occurred, then the initial breakdown will occur at the particle/matrix interface. The crack would grow at both ends of the craze and join in the center between the two particles, as shown schematically in Figure 3. The critical crack opening displacement δ_c at the crack tip calculated just prior to the final craze breakdown (i.e., as the crack length “ a ” goes to $\frac{1}{2}$ the interparticle distance λ) is given by

$$\delta_c = \frac{4}{\pi} \frac{(K_{1c})^2}{\sigma_y E} = \frac{4}{x} \frac{A \sigma_f'^2 \pi a}{\sigma_y E} = \frac{4A \sigma_f'^2 a}{\sigma_y E} \quad (1)$$

or

$$\delta_c = \frac{4AB^2 \sigma_f'^2 a}{\sigma_y E} \quad (2)$$

where K_{1c} = critical stress intensity factor; σ_y , yield stress; E , Young’s modulus; σ_f' , fibril stress at break; B , proportionality constant relating the macroscopic stress; (σ_f) and fibril stress (σ_f'); a , crack length;



δ_c = critical crack opening displacement
 a = crack length at breakdown
 λ = interparticle distance

Figure 3 Schematic of crack formation in crazed region between two rubber particles.

and A , constant (takes into account crack geometry and location).

In general, the energy to break (W) of a material may be determined from the area under the stress (σ)-strain (ϵ) curve, as expressed by

$$W = \int_0^{\epsilon_f} \sigma d\epsilon \quad (3)$$

where ϵ_f is the strain at fracture and $d\epsilon$ is an incremental increase in strain. In the simplest case of a completely elastic material or when the fracture is brittle, W is given by

$$W = \frac{1}{2} \sigma_f \epsilon_f \quad (4)$$

where σ_f is the stress at fracture. However, the modulus for a completely elastic material is defined as

$$E = \frac{\sigma_f}{\epsilon_f} \quad (5)$$

and by substituting (5) into (4),

$$W = \frac{\sigma_f^2}{2E} \quad (6)$$

By substituting eq. (6) into (2) and since δ_c and the yield stress are constant for a given polymer, then the energy to break is

$$W = \phi \left(\frac{1}{a} \right) \quad (7)$$

where

$$\phi = \frac{\delta_c \sigma_y}{8AB^2} \quad (8)$$

Since the interparticle distance = $2a$ (see Fig. 3), the breaking energy is proportional to (interparticle distance) $^{-1}$.

It can be shown that the mean free average distance between uniformly distributed particles in a matrix can be related to the volume fraction by²⁵

$$\bar{\lambda} = \frac{2}{3} d \left(\frac{V_m}{V_r} \right) \quad (9)$$

where V_r = volume of rubber particles of diameter d ; V_m , volume of matrix; λ , average interparticle distance; and d , particle diameter.

The above analysis allows qualitative prediction of the results. In Figure 4, the notched and un-

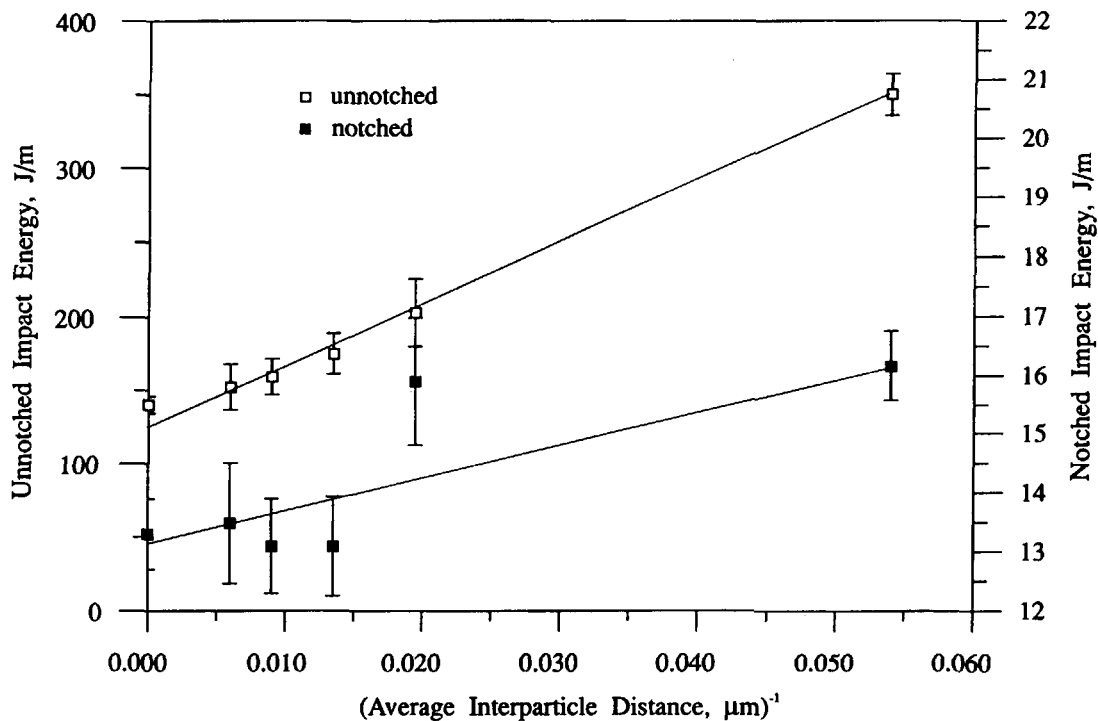


Figure 4 Impact energy (J/m) vs. (average interparticle distance, μm) $^{-1}$ for notched and unnotched Charpy specimens of 2.4 μm particle composites. Errors bars represent 95% confidence limit.

notched impact energy is plotted against (average interparticle distance)⁻¹ for 2.4 μm particles. The interparticle distance was varied by changing the proportion of rubber from 1 to 8 wt (or vol) %. Although both unnotched and notched tests show the same linear trend, the unnotched test results had less scatter. Therefore, the unnotched impact energy results only are used for further discussion. In the plot, the matrix impact energy corresponds to a material with infinite particle separation. The correspondence of toughness to interparticle spacing has been seen in other studies. Vu-Khanh²⁶ examined glass- and mica-reinforced polypropylene and noted the same inverse relationship.

The effect of particle size itself is shown in Figure 5 using the 8 rubber wt % data from Figure 2 and additional 2 and 4 rubber wt % data for the 6.2 μm particle composites. A change in particle size results in plots of different slopes, with the larger diameter particles being more effective than the smaller particles for a given interparticle spacing. A possible reason for this behavior is the ability not only to initiate more crazes at the surface of the largest particles but also to be more effective craze breakdown barriers (e.g., see TEM photographs by Keskkula et al.²⁷). Therefore, for any given interparticle spac-

ing, the amount of crazing is increased and, thus, the impact energy. In Figure 6, plots of interpolated impact energies from Figure 5 for constant interparticle distance for particle sizes $> 2 \mu\text{m}$ are given. A linear relationship is seen, with impact energy of "zero" particle size close to that of the matrix polystyrene.

Thus, for a given interparticle spacing, large diameter particles are more effective than are small particles. On the other hand, for a given particle size, the impact energy increases with a decrease in interparticle spacing in the matrix. Since the particle spacing is closer for smaller particles for a given rubber content [eq. (9)], these two trends combine to give the maximum seen in the impact energy in Figure 2. Note that the maximum will shift as the slopes in Figure 5 vary as rubber-matrix adhesion, rubber modulus, and other impact factors change. The model derived in this paper has validity for impact fracture of HIPS as well. Cigna et al.²⁸ obtained data on impact toughening on polystyrene-diluted HIPS blends with varying average rubber particle diameter. In Figure 7, the HIPS impact data is plotted against inverse interparticle distance and it can be seen that a linear relationship is followed.

Recently, a bimodal rubber particle distribution

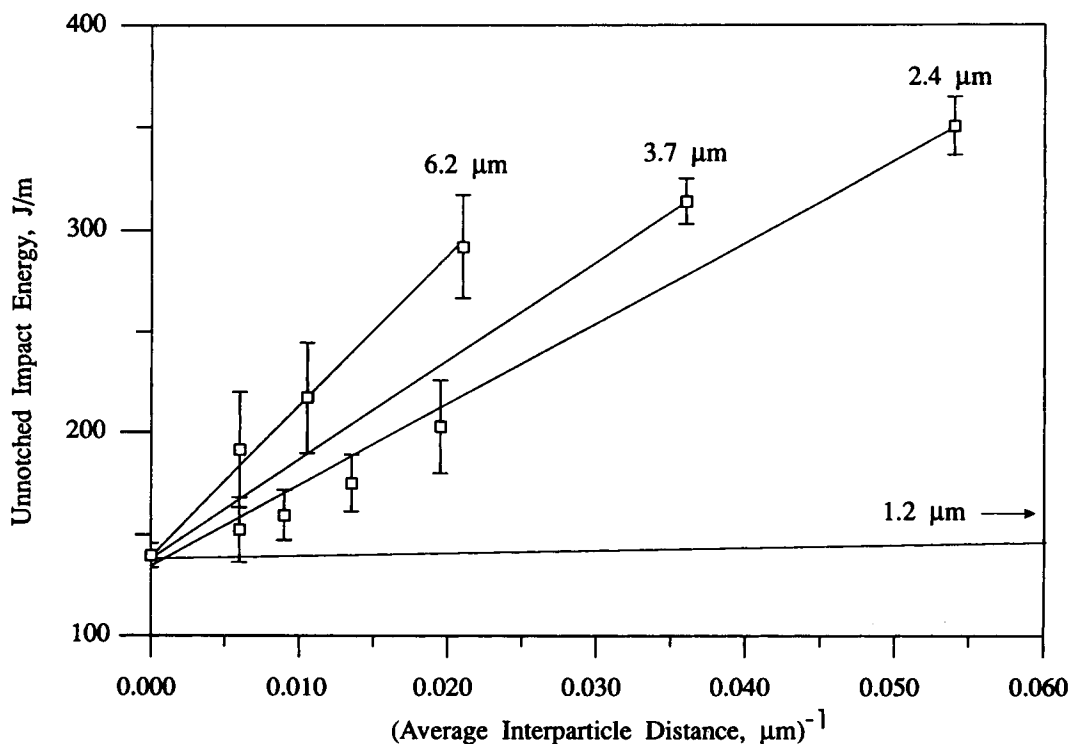


Figure 5 Impact energy (J/m) vs. (average interparticle distance, μm)⁻¹ for unnotched Charpy specimens of 6.2, 3.7, 2.4, and 1.2 μm particle composites.

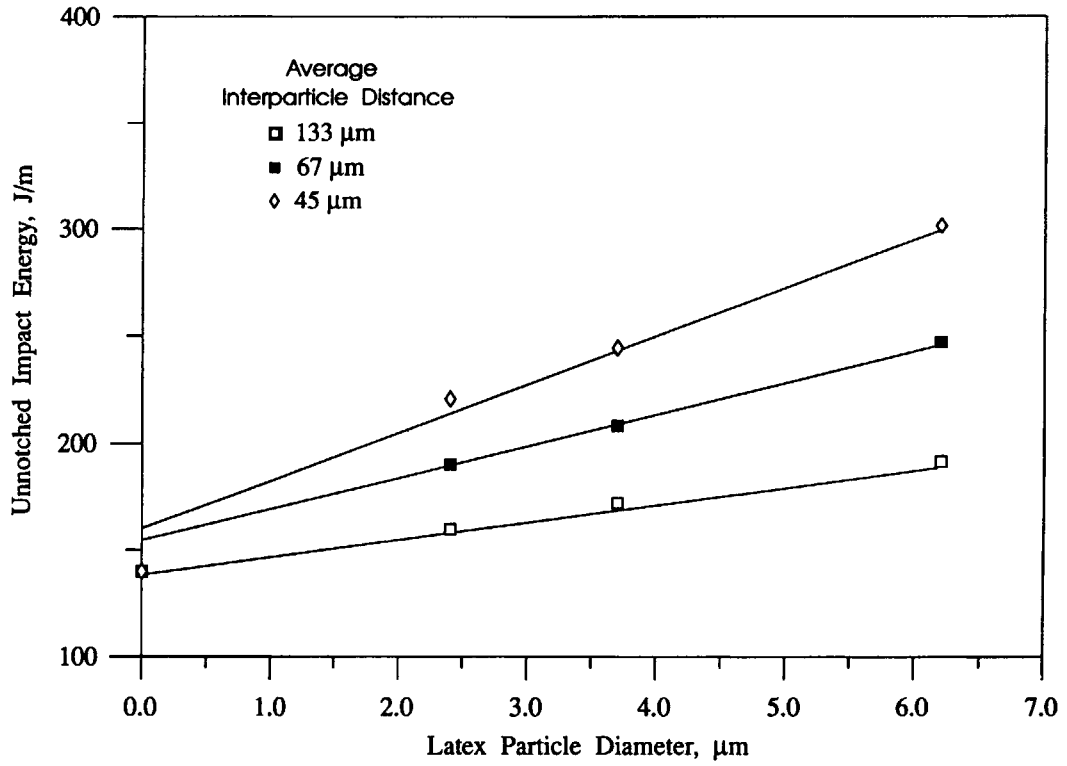


Figure 6 Unnotched impact energy as a function of particle size for different interparticle spacings. Data interpolated from Figure 5.

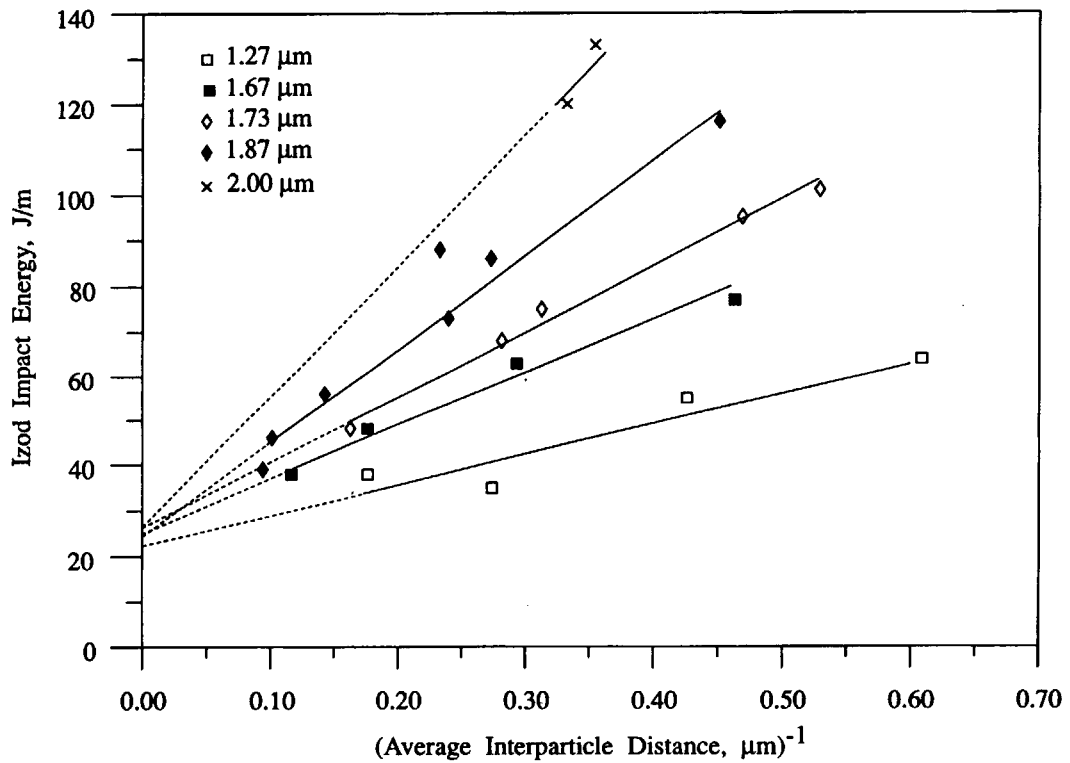


Figure 7 Plot of Izod impact energy (J/m) vs. (average interparticle distance, μm)⁻¹ spacing for HIPS/polystyrene blends of varying rubber particle size. Data from Cigna et al.²⁸ Interparticle distance calculated using eq. (9).

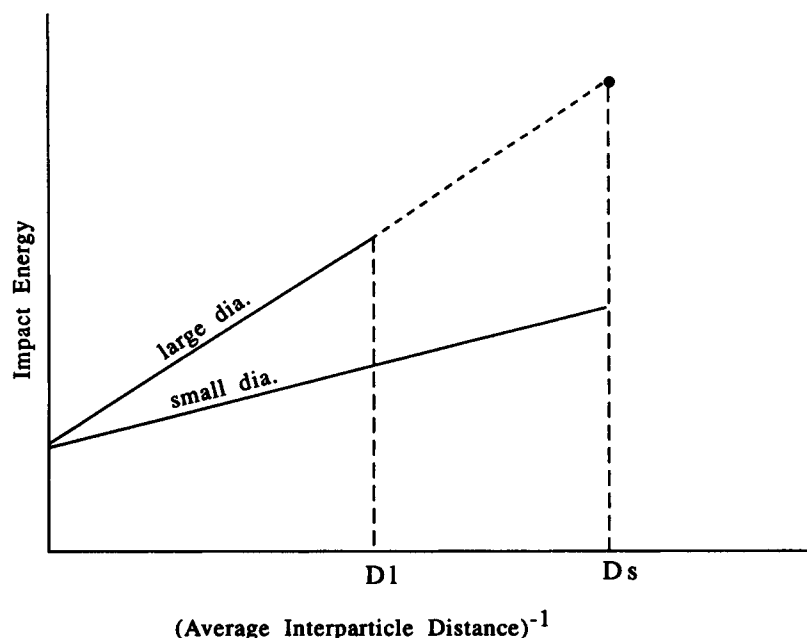


Figure 8 Schematic representation of Figure 5 for a bimodal particle distribution of small and large diameter particles, showing synergistic improvement in impact energy. D_l and D_s are the inverse particle spacings based on the large and small diameter particles, respectively.

with a population of small and large particles in HIPS has been shown to be more effective than a monomodal distribution.¹⁸ With respect to this model, the large particle impact energy vs. (average interparticle distance)⁻¹ plot is extended to intersect the interparticle spacing based on the smaller particles, and as a result, the impact energy will be higher than either, as shown schematically in Figure 8.

SUMMARY

The results suggest that large rubber particles ($> 2 \mu\text{m}$) are necessary for both initiating and controlling craze breakdown in polystyrene. The latter is the most important factor in the impact energy of the composites. The particles serve as barriers for the crazes, and a critical crack opening displacement model was developed to determine the impact energy dependence on particle diameter. The model predicts that the energy for fracture is proportional to the reciprocal of the spacing between particles and this was observed. It is postulated that the barrier efficiency depends on rubber-matrix adhesion, rubber cross-linking, and other factors that will be examined in a later paper.

The authors would like to take this opportunity to thank Dow Chemical Canada, Dow Chemical USA, and the Na-

tional Science and Engineering Research Council for financial support.

REFERENCES

1. C. B. Bucknall, *Toughened Plastics*, Applied Science, London, 1977, p. 187.
2. C. B. Bucknall and R. R. Smith, *Polymer*, **6**, 437 (1965).
3. C. B. Bucknall and D. Clayton, *J. Mater. Sci.*, **7**, 202 (1972).
4. C. G. Bragaw, *Adv. Chem. Ser.*, **99**, 86 (1971).
5. J. N. Goodier, *J. Appl. Mech.*, **55**, 39 (1933).
6. R. E. Lavengood, L. Nicolais, and M. Narkis, *J. Appl. Poly. Sci.*, **17**, 1173 (1973).
7. J. D. Moore, *Polymer*, **12**, 478 (1971).
8. D. G. Cook, A. Rudin, and A. Plumtree, *J. Appl. Polym. Sci.*, **46**, 1387 (1992).
9. S. L. Rosen, *J. Elastoplast.*, **2**, 195 (1970).
10. D. G. Cook, A. Plumtree, and A. Rudin, *Polym. Eng. Sci.*, **30**(10), 596 (1990).
11. C. Wrotecki, P. Heim, and P. Gaillard, *Poly. Sci. Eng.*, **31**(4), 213 (1991).
12. C. B. Bucknall, *Toughened Plastics*, Applied Science, London, 1977, p. 157.
13. S. Wu, *Polymer*, **26**, 1855 (1985).
14. T. A. Grocela and E. B. Nauman, *Polym. Mater. Sci. Eng.*, **63**, 488 (1990).
15. I. Narisawa, T. Kuriyama, and K. Ojima, *Makromol. Chem. Macromol. Symp.*, **41**, 87 (1991).

16. A. M. Donald and E. J. Kramer, *J. Appl. Polym. Sci.*, **27**, 3729 (1982).
17. A. M. Donald and E. Kramer, *Philos. Mag.*, **434**, 857 (1981).
18. Y. Okamoto, H. Miyagi, M. Kago, and K. Takahashi, *Macromolecules*, **24**, 5639 (1991).
19. A. M. Donald and E. J. Kramer, *J. Mater. Sci.*, **17**, 2351 (1982).
20. O. S. Gebizlioglu, H. W. Beckman, A. S. Argon, R. E. Cohen, and H. R. Brown, *Macromolecules*, **23**(17), 3968 (1990).
21. C. B. Bucknall and D. Clayton, *J. Mater. Sci.*, **7**, 202, (1972).
22. C. B. Bucknall, *Toughened Plastics*, Applied Science, London, 1977, p. 183.
23. D. Hull, *J. Mater. Sci.*, **5**, 357 (1970).
24. S. Y. Hobbs, *Polym. Eng. Sci.*, **26**(1), 74 (1986).
25. E. E. Underwood, *Quantitative Stereology*, Addison-Wesley, Reading, MA, 1970, p. 83.
26. T. Vu-Khanh, *J. Thermoplast. Compos. Mater.*, **4**, 46 (1991).
27. H. Keskkula, M. Schwarz, and D. R. Paul, *Polymer*, **27**, 211 (1986).
28. G. Cigna, C. Maestrini, L. Castellani, and P. Lomellini, *J. Appl. Poly. Sci.*, **44**, 505 (1992).

Received December 13, 1991

Accepted June 8, 1992